

## **Supporting Information**

### **A Simple, Sensitive and Rapid Voltammetric Detection of Alloxan on Glassy Carbon Electrode**

**Mallappa Mahanthappa<sup>a</sup>, Venkatesan Manju<sup>a</sup>, Anugraha Madamangalam Gopi<sup>c</sup>,  
Palaniappan Arumugam<sup>ab\*</sup>**

<sup>a</sup>Electrodes and Electrocatalysis Division, CSIR-Central Electrochemical Research Institute (CSIR-CECRI), Karaikudi-630003, India.

<sup>b</sup>Academy of Scientific and Innovative Research (AcSIR), Ghaziabad, Uttar Pradesh- 201 002.

<sup>c</sup>PG & Research Department of Chemistry, Sree Vyasa NSS College, Wadakkanchery, Thrissur, Kerala-680582, India.

<sup>†</sup>*Corresponding author E-mail:* [palani112@gmail.com](mailto:palani112@gmail.com), [palaniappan@cecri.res.in](mailto:palaniappan@cecri.res.in)

## Figure captions and Figures

**Scheme S1.** Synthesis of alloxazine.

**Figure S1.**  $^1\text{H-NMR}$  spectrum of alloxazine.

**Figure S2.**  $^{13}\text{C-NMR}$  spectrum of alloxazine.

**Figure S3.** FT-IR spectra of OPD (**Blackline**), Alloxan (**Redline**), Alloxan + OPD = Alloxazine formed *in-situ* (**Blueline**), and Alloxazine from chemical synthesis (**Pink line**).

**Figure S4.** UV-Visible absorption spectra of chemically synthesized alloxazine (**Blackline**) and *in-situ* prepared alloxazine (**Redline**) in 0.1 M NaOH.

**Figure S5.** Cyclic voltammograms of *in-situ* prepared alloxazine adduct (**Blackline**) and pure alloxazine (**Redline**) in 0.1 M NaOH on unmodified GCE at  $50\text{ mVs}^{-1}$ .

**Figure S6.** The plot of peak current vs. scan rate.

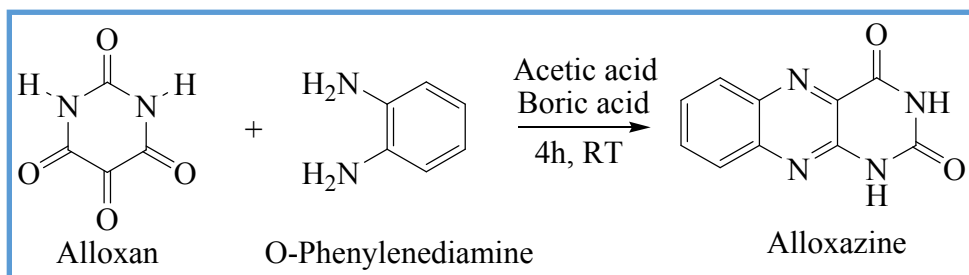
**Figure S7.** Effect of pH on the current response of alloxazine on an unmodified GCE.

**Figure S8 (a)** UV-Vis absorption spectra of freshly prepared alloxazine (*in-situ* method) adduct (**Blackline**) and after 4 h (**Redline**), **(b)** Absorption spectra of freshly prepared OPD solution (**Blackline**) and OPD after 24 h (**Redline**) **(c)** Absorption intensity vs. the effect of varying concentration of alloxan in the presence of fixed OPD concentration. Absorption spectra plotted after 24 h. The circle in the figure represents the degradation of the unreacted OPD after 24 h of the commencement of the reaction.

**Figure S9 (a)** Cyclic voltammetry response of *in-situ* formed alloxazine in (i)  $\text{O}_2$  saturated acetate buffer, (ii) acetate buffer with dissolved oxygen, and (iii)  $\text{N}_2$  saturated acetate buffer. **(b)** Bar diagram representing the variation in the current response under different acetate buffer conditions.

## Synthesis of Alloxazine

The alloxazine was synthesized by reported method<sup>1</sup>. Briefly, 4.764 mM (514 mg) of o-phenylene diamine was dissolved in 5 mL of glacial acetic acid. 4.997 mM (800 mg) of alloxan and 9.7 mM (600 mg) of powdered boric acid was dissolved in 10 mL of glacial acetic acid. The above two solutions were mixed and stirred for 4 h. The progress of the reaction was monitored by thin-layer chromatography. After the completion of the reaction, the product was extracted by using dichloromethane (DCM).



**Scheme S1.** Synthesis of alloxazine.

## Characterizations

<sup>1</sup>H-NMR (400 MHz, DMSO-d<sub>6</sub>) spectrum of alloxazine:  $\delta$  = 11.91 (s, 1H), 11.7 (s, 1H), 8.22 (d, J = 1.9 Hz, 1H), 7.93 (m, J = 8.8 Hz, 2H), 7.82 (d, J = 1.9, 8.8 Hz, 1H) and other peaks related DMSO. Final yield: 97%.

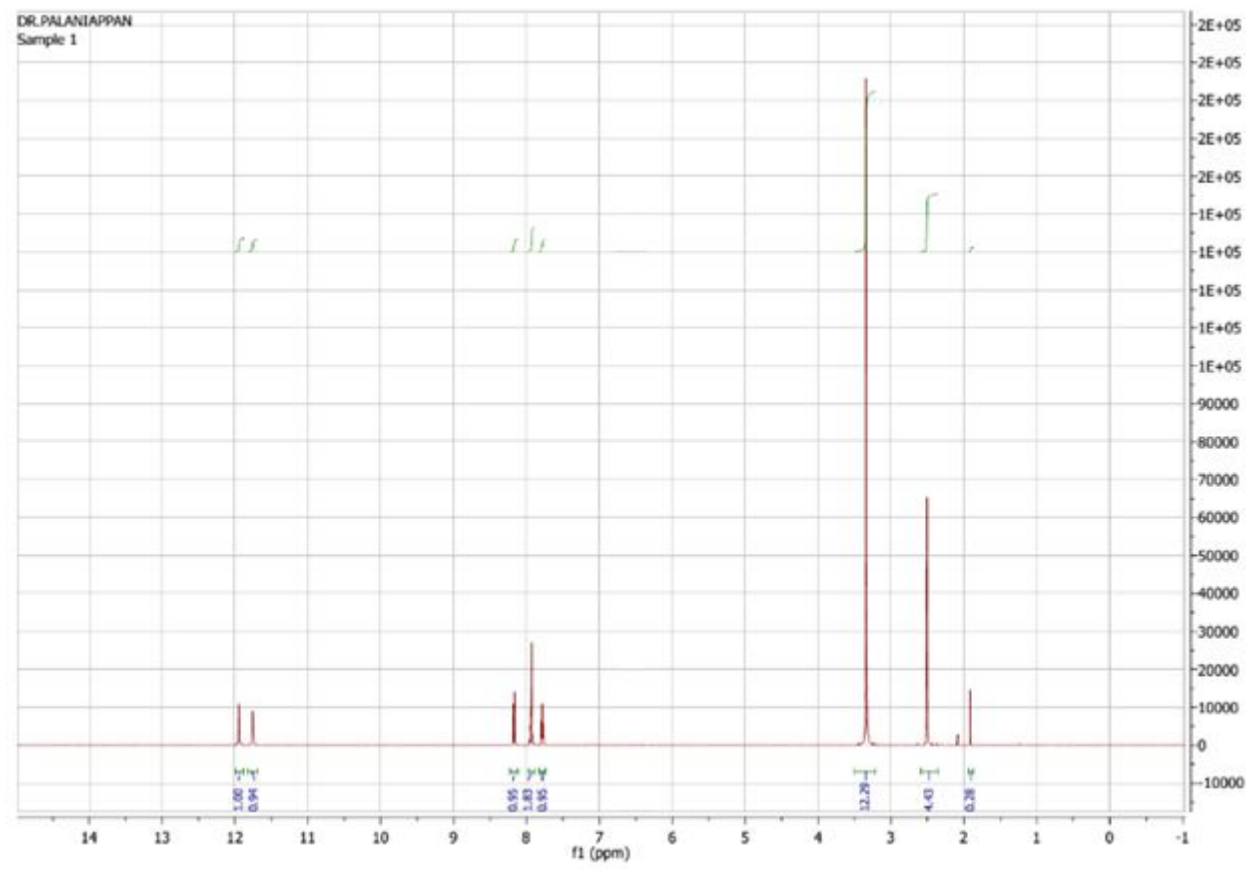


**Figure S1.** <sup>1</sup>H-NMR spectrum of alloxazine.

**<sup>13</sup>C-NMR (400 MHz, DMSO-d<sub>6</sub>) spectrum of alloxazine:  $\delta = 161, 150, 147, 143, 139, 133, 132, 130, 128, 127$ .**

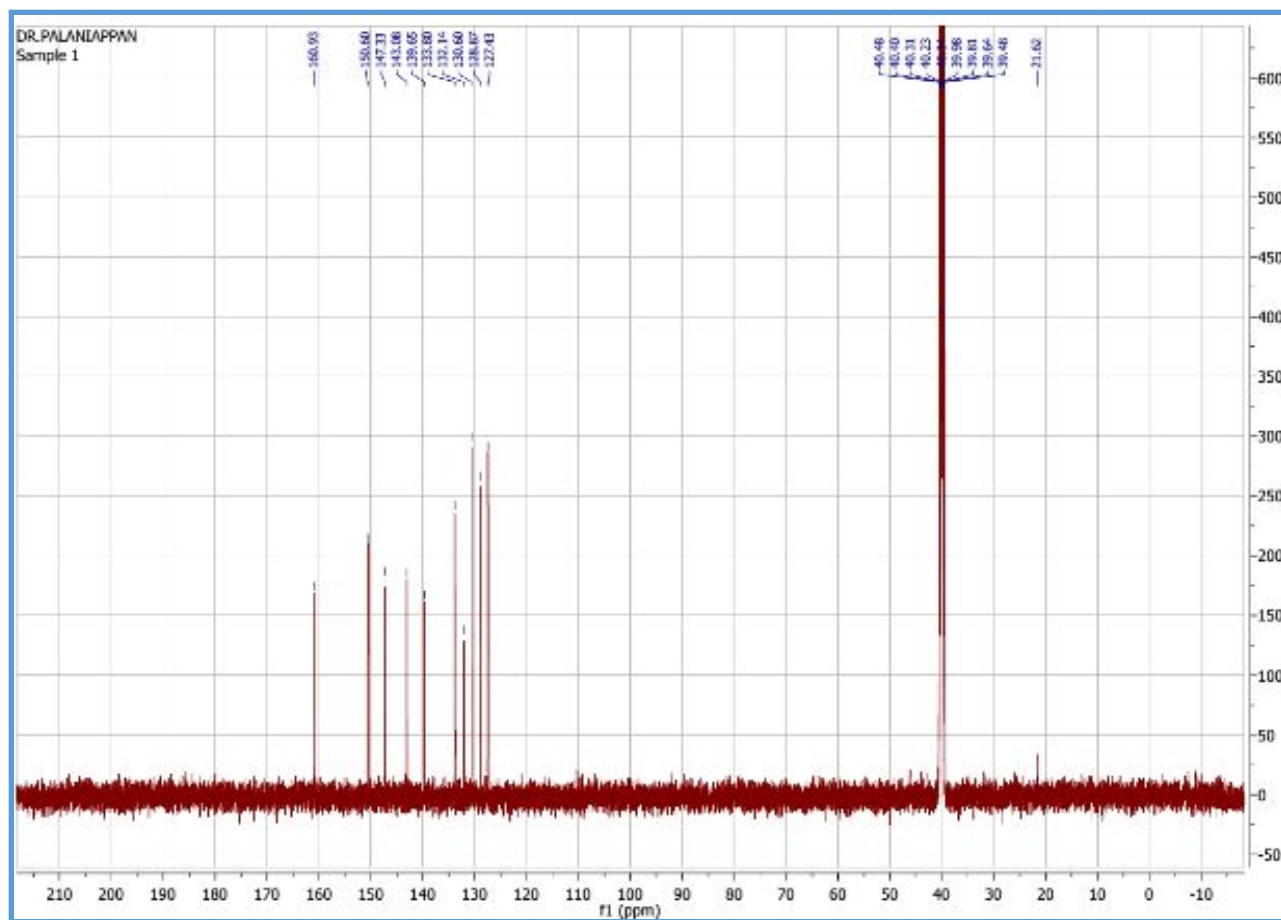


**Figure S2.** <sup>13</sup>C-NMR spectrum of alloxazine.

## FT-IR analysis of alloxazine

FT-IR spectrum of the alloxan, OPD and alloxazine were shown in **Figure S2**. The o-phenylene diamine shows peaks corresponding to that of aromatic C=C at around 1500  $\text{cm}^{-1}$ , peak at 1280  $\text{cm}^{-1}$  corresponds to C-N bond and peaks in the range of 3500-3000  $\text{cm}^{-1}$  indicate the presence of  $-\text{NH}_2$  functional groups. The alloxan shows a broad peak at 3250  $\text{cm}^{-1}$  which corresponds to hydrogen bonding of  $-\text{N}-\text{H}$  and  $-\text{O}-\text{H}$  groups. It also exhibits a peak at 1700  $\text{cm}^{-1}$  corresponding to C=O (keto) while the new peak was observed in the FT-IR spectrum of alloxazine at 1600  $\text{cm}^{-1}$  which confirms the formation of alloxazine adduct when reacting alloxan with OPD.

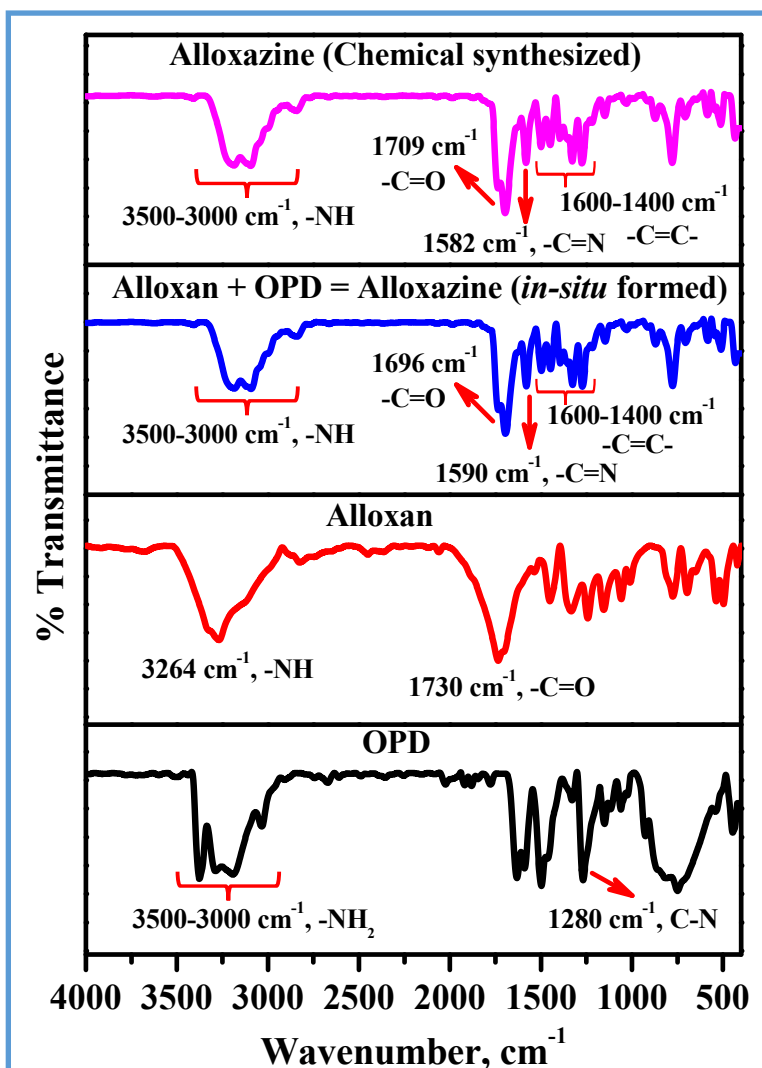


**Figure S3.** FT-IR spectra of OPD (**Blackline**), Alloxan (**Redline**), Alloxan + OPD = Alloxazine formed *in-situ* (**Blueline**), and chemically synthesized alloxazine (**Pink line**).

### UV-Visible absorption analysis of alloxazine (as prepared and *in-situ* formed)

The adduct formation in an *in-situ* reaction is confirmed to be alloxazine by comparing its UV-Vis spectrum with the UV-Vis spectrum of alloxazine prepared via chemical route. **Figure S4** represents the UV-Visible absorption spectra of both the *in-situ* product (**Redline**) and product from the chemical route (**Blackline**) in 0.1 M NaOH. Both the product exhibits similar absorption peaks at 226 nm, 244 nm, 260 nm, 271 nm, 333 nm, 372 nm and 423 nm in 0.1 M NaOH<sup>2</sup> confirms that the *in-situ* product is also an alloxazine only.

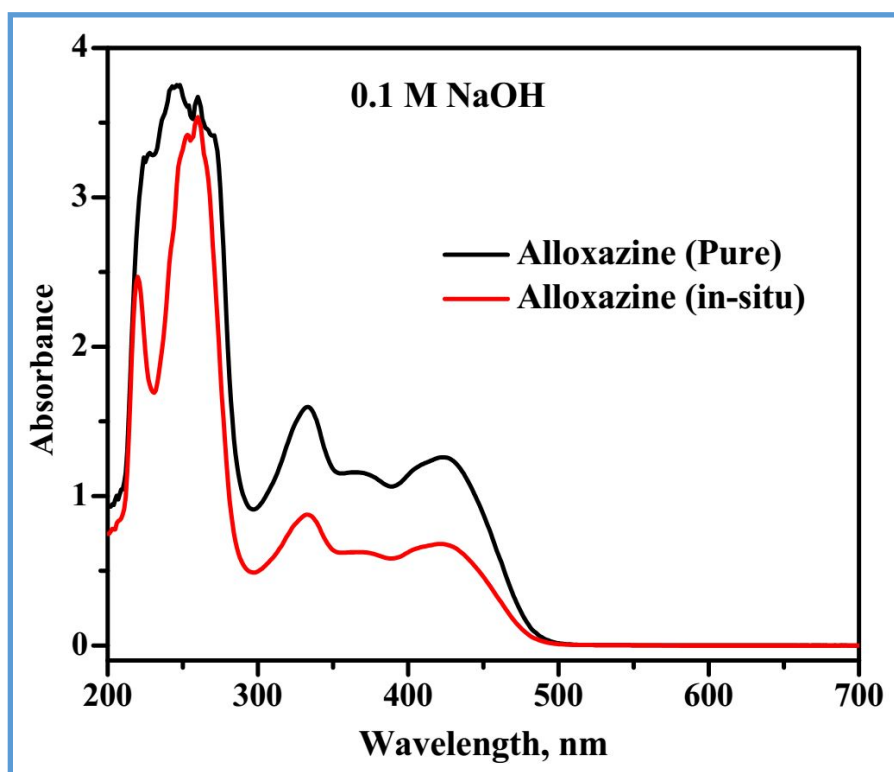


**Figure S4.** UV-Visible absorption spectra of chemically synthesized alloxazine (**Blackline**) and *in-situ* prepared alloxazine (**Redline**) in 0.1 M NaOH.

### Electrochemical conformation of *in-situ* formed alloxazine

Electrochemical behavior of alloxazine prepared via chemical routes and *in-situ* formed alloxazine were characterized using cyclic voltammetry in 0.1 M NaOH at 50 mVs<sup>-1</sup>. Blackline in **Figure S5** represents the cyclic voltammograms of chemically prepared alloxazine while the CV of *in-situ* prepared alloxazine adduct is represented in redline. It is evident from the figure that both the *in-situ* formed and chemically prepared alloxazine exhibits a well-defined redox peak at -0.84 V (cathodic) and -0.74 V (anodic) on an unmodified GCE in the potential range -0.2 to -1.0 V. It is well-known that in alkaline condition, the redox peak arises due to alloxazine undergo tautomerization to form isoalloxazine. Thus the *in-situ* prepared alloxazine adduct exhibits similar electrochemical behavior as that of chemically formed alloxazine.

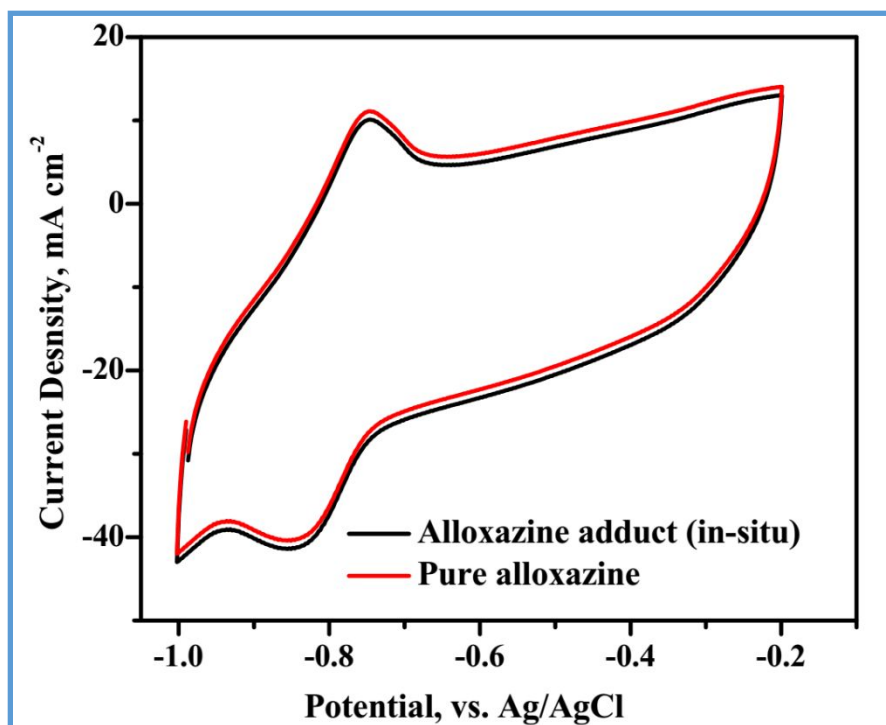


**Figure S5.** Cyclic voltammograms of *in-situ* prepared alloxazine adduct (**Blackline**) and pure alloxazine (**Redline**) in 0.1 M NaOH on an unmodified GCE at 50 mVs<sup>-1</sup>.



### Relationship between the scan rate and current

The plot of peak current ( $I_{pc}$ ) vs. scan rate ( $v$ ) is depicted in **Figure S6**. The peak current increases linearly with the scan rate, indicating that the electrode reaction process is adsorption controlled.

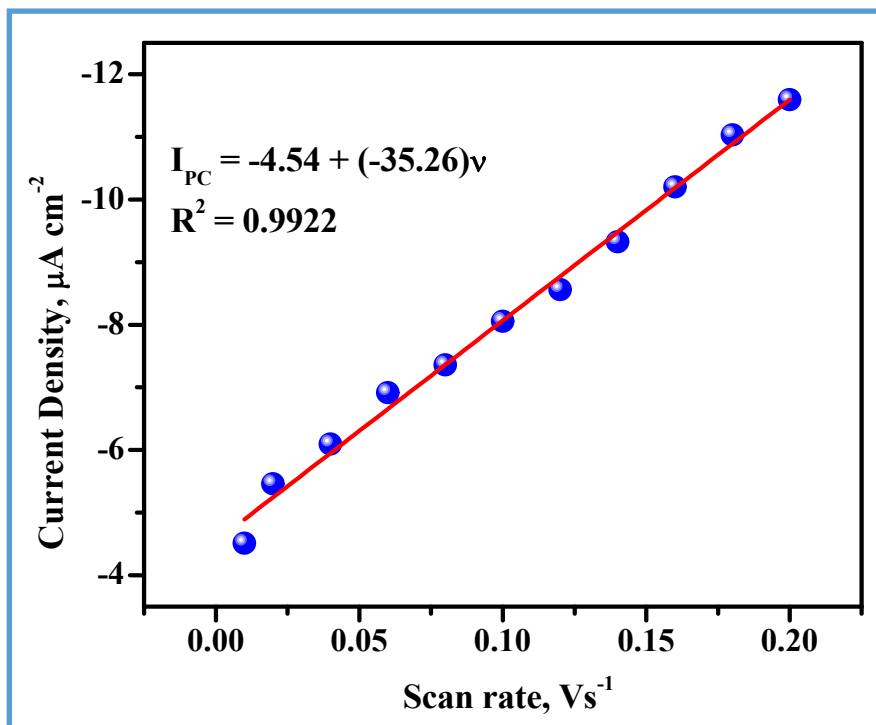


**Figure S6.** The plot of peak current vs. scan rate.

### Optimization of pH

The effect of pH plays an important role in the electrochemical behavior of alloxazine. **Figure S7** represents the effect of pH on the current response of alloxazine on an unmodified GCE in presence of acetate buffer solution with pH ranges from 3.5 to 5.5. Among these pH, a better current response was observed at pH 5.0 while a well-defined reduction peak was observed at pH 4.0 and 5.0. However, high purity of alloxazine adduct with good yield was obtained at pH 4.0. Hence, the pH 4.0 solution was chosen for further studies.

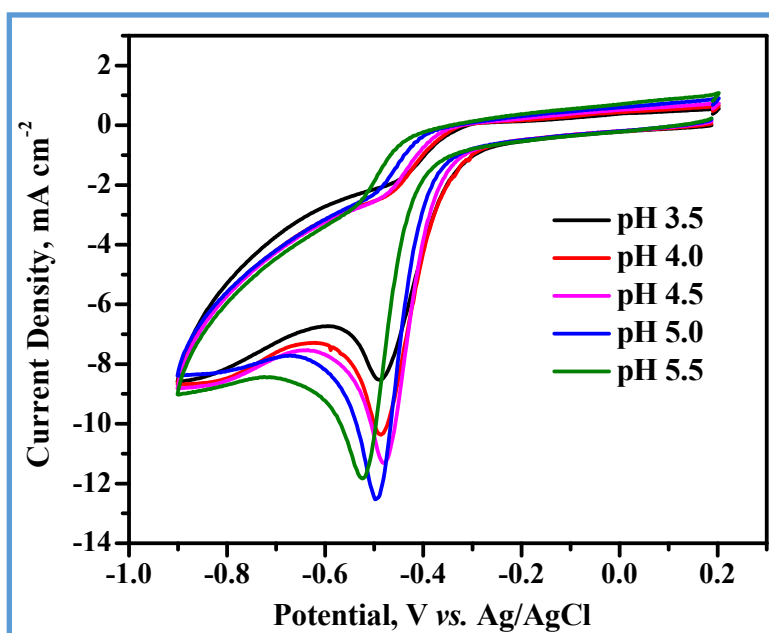


**Figure S7.** Effect of pH on the current response of alloxazine on unmodified GCE.

### Stability of alloxazine in the presence of OPD

Under optimized conditions, the stability of *in-situ* formed alloxazine was carried out by UV-Visible absorption spectroscopy. UV-Visible absorption spectra of 300  $\mu\text{M}$  alloxan in the presence of OPD (fresh and after 4 h *in-situ* formed alloxazine) in acetate buffer at pH 4.0 is represented in **Figure S8 (a)**. The absorption intensity of the alloxazine did not vary significantly even after 4 h which indicates the adduct stability over a period in contrast to alloxan whose half-life is a few seconds. Similarly, the stability of OPD was also studied and is shown in **Figure S8 (b)**. There is no characteristic absorption peak for fresh OPD solution (**Blackline**) and after 24 h (**Redline**), the OPD shows a strong absorption peak at 420 nm which may arise due to the photosensitive nature of OPD. A series of concentrations of alloxan (10 – 600  $\mu\text{M}$ ) was added into 1 mM OPD in acetate buffer (pH 4.0) and allowed to react for 24 h at room temperature. Thus obtained colorimetric assay is displayed in **Figure S8 (C)**. Upon the incremental addition of alloxan (10 to 600  $\mu\text{M}$ ) into 1 mM OPD, the absorption intensities at 315 nm and 382 nm increased gradually which signifies the formation of alloxazine adduct. However, the new absorption peak at 420 nm appeared due to the unreacted degraded OPD in the solution. Such observation is not noticed for the *in-situ* preparation of alloxazine adduct that was carried out within 4-5 hrs.

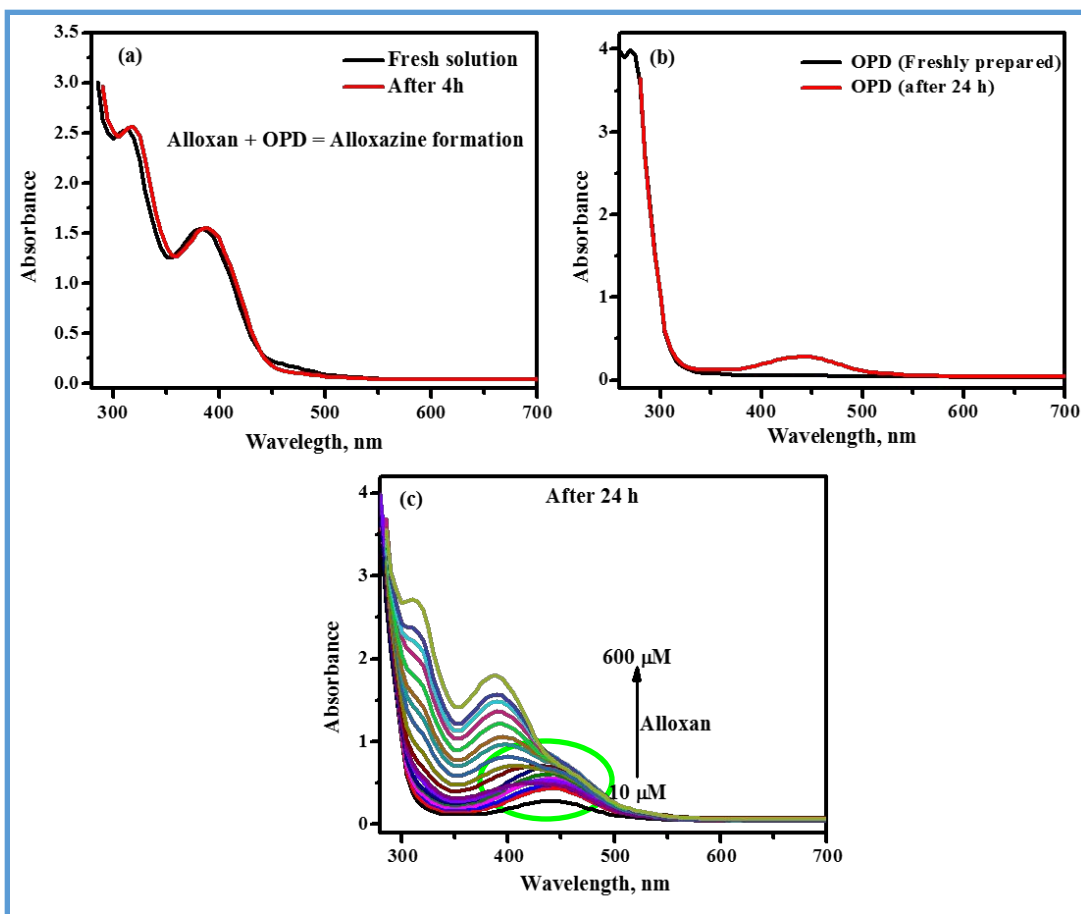


**Figure S8 (a)** UV-Vis absorption spectra of freshly prepared alloxazine (*in-situ* method) adduct (**Blackline**) and after 4 h (**Redline**), **(b)** Absorption spectra of freshly prepared OPD solution (**Blackline**) and OPD after 24 h (**Redline**) **(c)** Absorption intensity vs. the effect of varying concentration of alloxan in the presence of fixed OPD concentration. Absorption spectra plotted after 24 h. The circle in the figure represents the degradation of unreacted OPD after 24 h of the commencement of the reaction.

### Effect of O<sub>2</sub> in reduction current

To find the effect of the presence of oxygen in the electrochemical measurements, CVs were performed on 0.1 M acetate buffer solution containing alloxan and OPD under different conditions.

**Figure S9** represents the cyclic voltammograms of above acetate buffer (i) in saturated O<sub>2</sub>, (ii) in

dissolved oxygen and (iii) in saturated N<sub>2</sub> conditions. From the figure, it is evident that there is a small decrease in the current in presence of O<sub>2</sub>, while an increase in peak current is noticed in the N<sub>2</sub> saturated condition. On average, the GCE exhibits 11±1 μA cm<sup>-2</sup> for the alloxazine adduct in acetate buffer with (i) O<sub>2</sub> saturated (ii) dissolved oxygen, and (iii) N<sub>2</sub> saturated. The deviation in the current density is ~ 1 μA cm<sup>-2</sup> and it turns out to be 91, 100, and 106 % respectively.

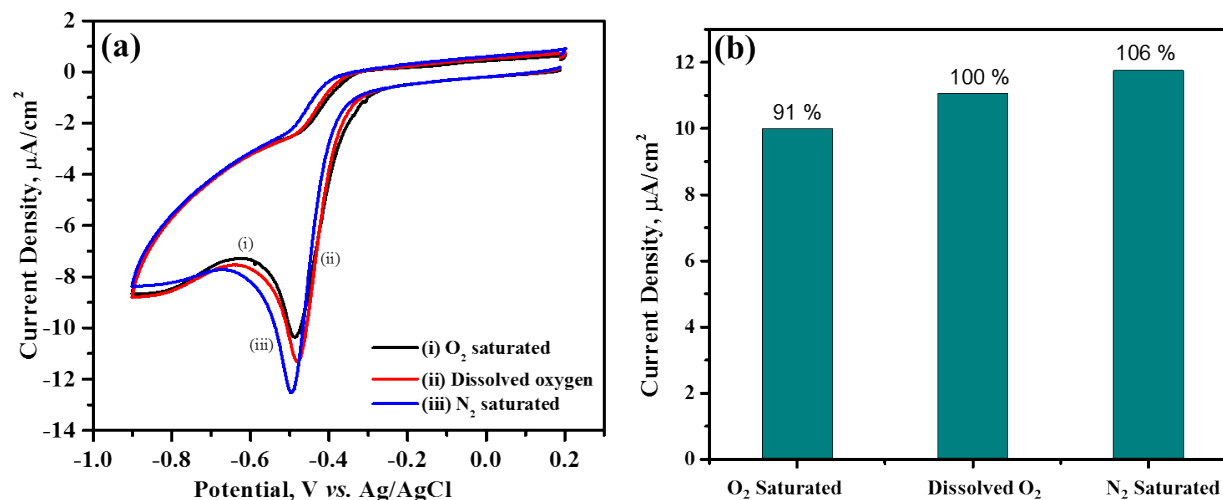


**Figure S9 (a)** Cyclic voltammetry response of *in-situ* formed alloxazine in (i) O<sub>2</sub> saturated acetate buffer, (ii) acetate buffer with dissolved oxygen, and (iii) N<sub>2</sub> saturated acetate buffer. **(b)** Bar diagram representing the variation in the current response under different acetate buffer conditions.

## References

1. Lin, K.; Gómez-Bombarelli, R.; Beh, E. S.; Tong, L.; Chen, Q.; Valle, A.; Aspuru-Guzik, A.; Aziz, M. J.; Gordon, R. G., A redox-flow battery with an alloxazine-based organic electrolyte. *Nat. Energy*. **2016**, *1* (9), 16102.
2. Penzkofer, A., Absorption and emission spectroscopic investigation of alloxazine in aqueous solutions and comparison with lumichrome. *J. Photochem. Photobiol. A*. **2016**, *314*, 114-124.